



The Predictive Role of Mammography, Dynamic Contrast-Enhanced Breast Magnetic Resonance Imaging and Diffusion-Weighted Imaging in Hormone Receptor Status of Pure Ductal Carcinoma *In Situ* Lesions

Almıla Coşkun Bilge¹, Zarife Melda Bulut²

¹Department of Radiology, Dr. Abdurrahman Yurtaslan Ankara Oncology Training and Research Hospital, Ankara, Turkey

²Department of Pathology, Dr. Abdurrahman Yurtaslan Ankara Oncology Training and Research Hospital, Ankara, Turkey

ABSTRACT

Objective: The aim of this retrospective study was to analyze the predictive capabilities of preoperative mammography, dynamic contrast-enhanced-magnetic resonance imaging (DCE-MRI), and diffusion-weighted imaging (DWI) in determining hormone receptor (HRc) status for pure ductal carcinoma *in situ* (DCIS) lesions.

Materials and Methods: The study included a total of 79 patients who underwent preoperative mammography (MG) and MRI between December 2018 and December 2023 and were subsequently diagnosed with pure DCIS after surgery. The correlation between MG, DCE-MRI, and DWI features and estrogen receptor (ER) and progesterone receptor (PR) status was examined.

Results: Among the lesions, 44 were double HRc-positive (ER and PR-positive), 13 were single HRc-positive (ER-positive and PR-negative or ER-negative and PR-positive) and 22 were double HRc-negative (ER and PR-negative). The presence of symptom ($p = 0.029$), the presence of comedo necrosis ($p = 0.005$) and high histological grade ($p < 0.001$) were found to be associated with ER and PR negativity. Amorphous microcalcifications were more commonly observed in the double HRc-negative group, while linear calcifications were more prevalent in both double and single HRc-positive groups ($p = 0.020$). Non-mass enhancement (NME) with a linear distribution was significantly more common in double HRc-negative lesions (38%), and NME with a segmental distribution in both double (43%) and single (50%) receptor-positive lesions ($p = 0.042$). Evaluation of DWI findings revealed that a higher lesion-to-normal breast parenchyma apparent diffusion coefficient (ADC) ratio statistically increased the probability of HRc positivity ($p = 0.033$).

Conclusion: Certain clinicopathological, mammography, and MRI features, along with the lesion-to-normal breast parenchyma ADC ratio, can serve as predictors for HRc status in DCIS lesions.

Keywords: Ductal carcinoma *in situ*; mammography; magnetic resonance imaging; diffusion-weighted MRI; estrogen receptor; progesterone receptor

Cite this article as: Coşkun Bilge A, Bulut ZM. The Predictive Role of Mammography, Dynamic Contrast-Enhanced Breast Magnetic Resonance Imaging and Diffusion-Weighted Imaging in Hormone Receptor Status of Pure Ductal Carcinoma *In Situ* Lesions. Eur J Breast Health. 2024; 20(4): 241-250

Key Points

- Ductal carcinoma *in situ* is a heterogeneous disease in terms of its histopathological features, which is a precursor to invasive breast cancer.
- Evaluation of hormone receptor status is important for preoperative treatment planning.
- The presence of symptoms, the presence of comedo necrosis, histological grade, microcalcification morphology, the distribution pattern of non-mass enhancement, and tumor-to-normal parenchyma apparent diffusion coefficient ratio may be considered valuable in preoperatively predicting hormone receptor status in cases of ductal carcinoma *in situ*.

Introduction

Ductal carcinoma *in situ* (DCIS) is recognized as a precursor to invasive breast cancer, comprising approximately 25-30% of all breast cancers today (1, 2). DCIS is a heterogeneous disease depending on its histopathological and biological features (2, 3). Molecular subtyping primarily relies on the analysis of hormone receptors (HRc), such as

estrogen receptor (ER) and progesterone receptor (PR) (2). The few published studies exploring the impact of molecular characteristics on prognosis in DCIS indicate that HRc-negative lesions tend to be associated with local recurrence (4, 5). The assessment of prognostic factors holds significance in guiding treatment management. Based on these evaluations, appropriate treatment strategies for DCIS

Corresponding Author:
Almıla Coşkun Bilge; almilacoskun@gmail.com

Received: 04.05.2024
Accepted: 15.06.2024
Available Online Date: 26.09.2024



are determined, encompassing surgical options (mastectomy/lumpectomy), radiation therapy, and adjuvant hormone therapy (1, 2, 5).

Core needle biopsies (CNBs) are regarded as the gold standard for preoperative breast tumor diagnosis. However, under sampling during CNBs and the highly heterogeneous internal pattern of DCIS lesions can contribute to pathologically uncertain interpretations (6). Radiological imaging methods play a crucial role in characterizing the entire tumor. Mammography (MG) is the primary imaging modality for diagnosing DCIS, with calcification being the dominant reported feature (7). ER-positive DCIS commonly present as fine pleomorphic and fine-linear branching calcifications (6). Additionally, the literature defines other findings, such as architectural distortions, masses, and focal densities (8). Dynamic contrast-enhanced-magnetic resonance imaging (DCE-MRI) provides high sensitivity for breast lesions (7). Preoperative MRI can provide essential data to reveal the extent of disease and assist in surgical management planning for DCIS cases (9). DCIS lesions typically manifest as clumped nonmass enhancement (NME) in a segmental or linear distribution, with plateau or washout kinetic curves (7, 10). While DCE-MRI reveals the morphology and vascularization of lesions, diffusion-weighted imaging (DWI) provides insights into tissue cellularity and the integrity of cell membranes. Quantitative evaluation of DWI features involves obtaining apparent diffusion coefficient (ADC) values from DWI images. DCIS lesions generally exhibit lower ADC values compared to normal breast tissue and benign lesions (11).

The potential heterogeneous distribution of antigens within DCIS lesions raises concerns about the accuracy of HRc profiling based on samples obtained via CNB, as they may not fully represent the complete tumor tissue (12). A non-invasive, biopsy-complementary method capable of assessing the entire lesion is thus important for predicting the presence of ER and PR in DCIS. Integrating preoperative MG and DWI into DCE-MRI protocols holds promise for differentiating the HRc status of DCIS lesions (13). However, it is noteworthy that there are fewer reports evaluating DCE-MRI and DWI findings according to HRc status in pure DCIS lesions compared to investigations focusing on MG findings (14, 15).

The aim of this study was to assess whether findings from MG, DCE-MRI and DWI can predict the HRc status in cases of pure DCIS.

Materials and Methods

This retrospective study received approval from the Non-Interventional Clinical Research Ethics Committee of Health Sciences University Turkey, Dr. Abdurrahman Yurtaslan Ankara Oncology Health Education Application and Research Center (no.: 2023-12/123, date: 14.12.2023), and informed consent was obtained from each participant.

Patients

Data from 489 patients histopathologically diagnosed with pure DCIS following breast-conserving surgery or mastectomy at our institute between December 2018 and December 2023 were retrospectively accessed from the electronic medical record archive. From this cohort, 124 patients with preoperative MG, DCE-MRI, and DWI images were identified in our radiology image archive. Exclusion criteria were applied to ensure the study's integrity, resulting in the exclusion of 45 patients. Reasons for exclusion included receiving

neoadjuvant chemotherapy or endocrine therapy ($n = 35$), having DWI images unsuitable for measuring the ADC value due to artifacts ($n = 6$), or having lesions smaller than 5 mm where region of interest (ROI) measurements were not feasible ($n = 4$). The final participant count in the study stood at 79. Clinical characteristics such as age, symptoms, risk factors, and histopathological features of the lesions were meticulously extracted from the patients' medical records.

Mammography Technique

MG was conducted using a digital MG system (LORAD, Hologic Company, Selenia Mammography System, Danbury, USA). Craniocaudal and mediolateral oblique views were acquired as part of the routine MG imaging process. For a more detailed assessment of low-density microcalcifications with ambiguous morphology and distribution in standard MG, a magnification view was employed, using a magnification factor of 1.8. A spot compression view, employing a compression paddle, was conducted to discern focal asymmetric densities or mass lesions visible in routine MG, distinguishing them from superpositions with surrounding tissue and enhancing visualization of lesion boundaries. The resulting images were presented on a pair of high-resolution 5-megapixel 21-inch LCD monitors (Coronis MDMG-5121, Barco, Belgium).

Mammography Findings

A radiologist with 13 years of experience in breast imaging conducted retrospective review of the MG images without access to the clinical information or pathological outcomes of the cases. Lesions were categorized into four groups based on mammographic findings: occult, mass, calcifications, and mass with microcalcifications. The morphological features of calcifications and masses, as well as the distribution of calcifications, were meticulously assessed using the American College of Radiology Breast Imaging Reporting and Data System (BI-RADS) lexicon (American College of Radiology, 2013) (16). The shape of the mass was described as either oval/round or irregular, with its margin defined as either circumscribed or indistinct/spiculated. Calcifications were morphologically classified as amorphous, coarse heterogeneous, fine pleomorphic, and fine linear/branching. The distribution of calcifications was subgrouped as regional, grouped, linear, and segmental. Following the comprehensive evaluation of the MG views, an MG-BI-RADS category was assigned to each case.

MRI Technique

MRI examinations were conducted using a 1.5-Tesla MR scanner (SignaHDx; GE Healthcare, Wisconsin, USA) with the patient positioned prone and with a dedicated breast coil. The MRI sequences and corresponding image parameters were as follows: Axial short tau inversion recovery [repetition time/echo time (TR/TE): 6500/45, inversion time: 150 ms, field of view (FOV): 320 mm, matrix: 416 × 224, number of excitations (NEX): 1, and slice thickness (ST): 5 mm]; axial T1-weighted (T1W) (TR/TE: 400/8.8, FOV: 320 mm, matrix: 448 × 224, NEX: 1, and ST: 5 mm); dynamic axial fat-saturated T1W (before and after contrast injection) (TR/TE: 4/1.5, flip angle: 10°, FOV: 320 mm, matrix: 350 × 350, NEX: 1, and ST: 2.8 mm); and echo-planar imaging-based DWI (TR/TE: 1000/83, FOV: 320 mm, matrix: 192 × 192, NEX: 4, ST: 5 mm, with b-values of 0 and 800 s/mm²). Each patient underwent one pre-contrast scan, and dynamic series comprising five post-contrast scans following intravenous administration of a contrast agent injection (0.1 mmol/kg gadobutrol/gadopentetate dimeglumine) at a dose of 0.1 mmol per kilogram

of body weight, followed by a 20 mL saline flush. Subtraction, multiplanar reconstruction, and maximum-intensity projection images were automatically generated on a dedicated workstation. Applying ROI drawing, ADC values were obtained. The ROI area was adjusted based on the lesion size, with a mean ROI size of 54 mm² (range, 35–110 mm²).

MRI Findings

The preoperative breast MRI images for all cases underwent retrospective review on a workstation by a radiologist with 13 years of experience in breast imaging. The radiologist conducted the analysis in a blinded manner, without access to clinical information or pathologic outcomes. MRI findings for each lesion were systematically analyzed following the BI-RADS MRI lexicon, encompassing morphological and enhancement features (16).

Lesion morphology was differentiated into mass and NME. For mass lesions, shape features were characterized as oval/round or irregular, while margin features were defined as circumscribed or not circumscribed (irregular and spiculated), in accordance with the BI-RADS MRI lexicon. NME lesion distributions were classified as focal, linear, segmental, or regional.

Internal enhancement patterns were categorized as homogeneous, heterogeneous, or rim for mass lesions, and as homogeneous, heterogeneous, clumped, or clustered ring for NME lesions. A time-intensity curve was automatically generated by placing the cursor on the most intensely and suspiciously enhanced areas of the lesions on postcontrast images. The obtained kinetic curves were scrutinized, and the contrast enhancement patterns were determined for both the initial phase (slow, medium, or rapid) and the delayed phase (persistent, plateau, or washout).

ADC value measurements were conducted in areas corresponding to the lesions identified in DCE-MRI images on ADC maps resulting from the processing of DWI images. Oval or round ROIs were drawn

on ADC maps for both the lesion and normal breast parenchyma (in the same quadrant as the lesion in the contralateral breast or in the ipsilateral breast in cases with contralateral mastectomy/lumpectomy) (Figure 1). Minimum ADC values were computed for the lesion and maximum ADC values for the normal tissue. The measured minimum ADC values of the lesions and the ratio of lesion ADC to normal parenchyma ADC were documented.

Pathological Evaluation

Lumpectomy or mastectomy materials underwent evaluation by a pathologist with 22 years of expertise in breast pathology. The assessment included determining tumor tissues through ER and PR staining, evaluating tumor viability, and ensuring the presence of a sufficient tumor area. Under light microscopy, nuclear ER and PR expression in areas of DCIS were examined in tissue samples. Tumors with $\geq 10\%$ nuclear staining were deemed receptor-positive. DCIS lesions were further categorized into three groups based on their immunohistochemical profile: Double hormone receptor-positive (ER-positive, PR-positive), single hormone receptor-positive (ER-positive, PR-negative or ER-negative, PR-positive), and double hormone receptor-negative (ER-negative, PR-negative). Furthermore, DCIS was stratified into low-, intermediate-, or high-grade. In addition, and following the College of American Pathologists protocol, the presence of comedo necrosis was defined. The pathology reports, encompassing the aforementioned information, were retrospectively obtained from the electronic medical archive of our hospital.

Statistical Analysis

Statistical analyses were executed using IBM SPSS software, version 20.0 (IBM Corporation, Armonk, NY, USA). Clinicopathological and radiological data were stratified based on the hormone receptor status of DCIS lesions, delineated as double positive (ER-positive/PR-positive), single positive (ER-positive/PR-negative or ER-negative/PR-positive), and double negative (ER-negative/PR-negative). Descriptive statistics, including mean, standard deviation, median, minimum,

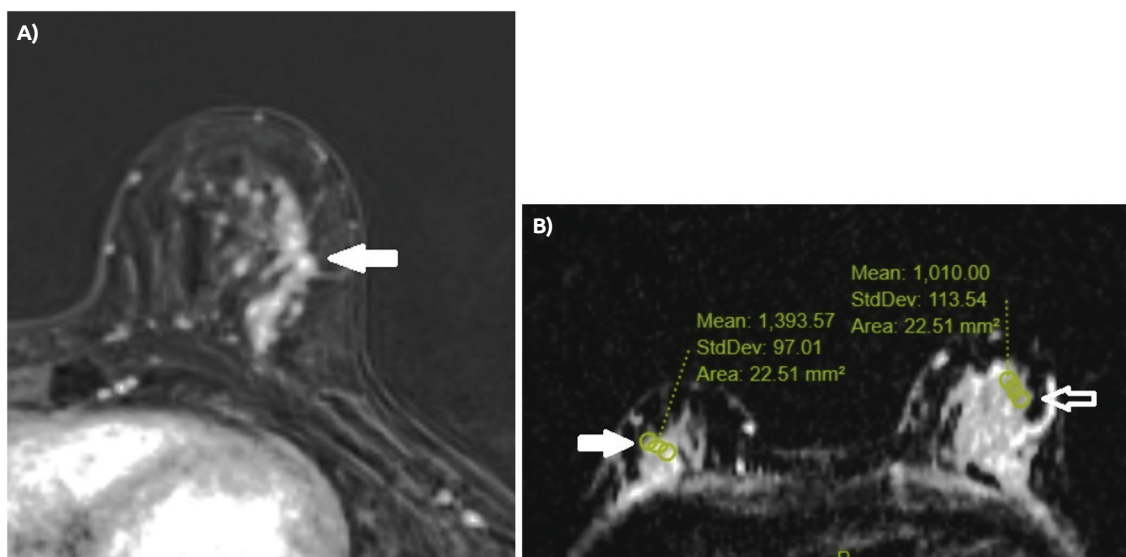


Figure 1. A 54-year-old woman with high-grade pure DCIS containing foci of comedo necrosis. Immunohistochemical analysis established that ER was positive and PR was negative. **A)** Axial postcontrast subtraction image showed a heterogeneous nonmass enhancement with segmental distribution in the left breast (arrow). **B)** ADC measurements were made from the lesion (empty arrow) and from the same quadrant as the lesion in the contralateral breast parenchyma (arrow) in the ADC map. The minimum lesion ADC value was $1010 \times 10^{-6} \text{mm}^2/\text{second}$, the maximum normal breast parenchyma ADC value was $1393 \times 10^{-6} \text{mm}^2/\text{second}$, and the lesion- normal breast parenchyma ADC ratio was 0.72

maximum, and percentages, were produced. For categorical variables, such as clinicopathological data, MG, and DCE-MRI findings, the chi-square test or Fisher exact test, if necessary, was employed to assess their association with the hormone receptor status of DCIS lesions. Normality analyses were conducted for continuous variables, including patient age, lesion size, lesion ADC value, and lesion-to-normal breast parenchyma ADC ratio, using the Kolmogorov-Smirnov goodness-of-fit test and Shapiro-Wilk test. To evaluate significant differences in continuous dependent variables between groups, the Kruskal-Wallis H test was used for lesion size, ADC value, and lesion-to-normal breast parenchyma ADC ratio, while One-Way ANOVA was employed for the patient age variable. A *p*-value less than 0.05 was considered statistically significant. The threshold value of the lesion/normal breast parenchyma ADC ratio was determined using receiver operating characteristic (ROC) analysis. The optimal cut-off for the lesion/normal parenchyma ADC ratio was determined with reference to the Youden index.

Results

Clinicopathological Features

In the histopathological assessment of 79 DCIS lesions, 44 were found to be ER and PR-positive, 13 were ER-positive and PR-negative or ER-negative and PR-positive, and 22 were ER and PR-negative. The mean age of the study participants was 50.96±12.14 years (range 24 - 79 years). Upon comparing the groups, no significant relationship was identified between the HRc status and patient age (*p* = 0.150). Patients over the age of 50 were distributed in the double HRc-positive, single HRc-positive, and double HRc-negative groups at rates of 45%, 46%, and 63%, respectively (*p* = 0.356). The rate of symptomatic patients in the ER and PR-negative group was 63%, which was significant. Specifically, the rate of symptomatic patients was 63% in the ER and PR-negative group, 29% in the ER and PR-positive group, and 38% in the single HRc-positive group (*p* = 0.029). No significant difference was observed between the groups regarding the presence of breast cancer risk factors (*p* = 0.556) (Table 1). The median histopathologically confirmed size of DCIS lesions was 25 mm (range 5 - 85 mm). The lesion size, even when subgrouped by 20 mm, did not exhibit statistically significant differences in intergroup comparisons (*p* = 0.556). Comedo necrosis was identified in 77% of ER and PR-negative lesions, 76% of single HRc-positive lesions, and 40% of ER and PR-positive lesions, showing a significant relationship with the HRc status of the DCIS lesions (*p* = 0.005). Moreover, DCIS with a high histological grade was predominantly found in the ER and PR-negative group (95%), followed by the single receptor-positive group (46%), and the ER and PR-positive group (43%) (*p*<0.001).

Mammography Findings

In each group, DCIS lesions predominantly manifested as microcalcifications on MG, with rates of 38% for the double HRc-positive group, 69% for the single HRc-positive group, and 31% for the double HRc-negative group (*p* = 0.348). The intergroup distribution of shape and margin characteristics of lesions in mass morphology is detailed in Table 2, revealing no statistically significant differences (*p* = 0.494, *p* = 1.000, respectively). Examining the distribution of microcalcification morphology between groups, fine pleomorphic microcalcifications were detected in 50% and 60% of the double and single HRc-positive groups, respectively, while amorphous microcalcifications were observed in 50% of the HRc-negative group (*p* = 0.020) (Figure 2). However, no significant correlation was found

between the distribution patterns of microcalcifications and the HRc status of the lesions (*p* = 0.856). MG BI-RADS category 4C was identified in 31% of double HRc-positive and HRc-negative lesions and 38% of single HRc-positive lesions, with no significant difference found between the groups (*p* = 0.998).

DCE-MRI Findings

In MRIs, the predominant lesion morphological types in the double HRc-positive, single HRc-positive, and double HRc-negative groups were NME in 84%, 92%, and 81%, respectively (*p* = 0.831). A single mass lesion was identified in the single HRc-positive group with an irregular shape and margin. For both ER and PR-positive and -negative groups, the dominant mass shape was round/ovoid (71% and 75%, respectively), while the predominant margin feature was irregular/spiculated (71% and 100%, respectively). There were no significant differences in the shape and margin characteristics of mass lesions between the groups (*p* = 0.463 and *p* = 0.576, respectively). While NME with a segmental distribution was commonly observed in both double (43%) and single (50%) HRc-positive lesions, NME with a linear distribution was more frequent in HRc-negative lesions (38%) (Figure 3). Statistically significant differences were found in the distribution of NME lesions between the groups *p* = 0.042. Regarding the internal enhancement pattern of NME, the clumped pattern was predominant in both double HRc-positive (51%) and negative (33%) lesions, while the heterogeneous enhancement pattern prevailed in single HRc-positive lesions (50%) (*p* = 0.186). The distribution of

Table 1. Clinicopathological features of the cases according to hormone receptor subgroups

	ER/PR positive (n) (%)	Single positive (n) (%)	ER/PR negative (n) (%)	<i>p</i> -value
Age (grouped)				
≤50 years	24 (54.5)	7 (53.8)	8 (36.4)	0.356
>50 years	20 (45.5)	6 (46.2)	14 (63.6)	
Symptom				
No	31 (70.5)	8 (61.5)	8 (36.4)	0.029
Yes	13 (29.5)	5 (38.5)	14 (63.6)	
Risk factors				
No	33 (75)	11 (84.6)	15 (68.2)	0.556
Yes	11 (25)	2 (15.4)	7 (31.8)	
Size (grouped)				
≤20 mm	20 (45.5)	4 (30.8)	9 (40.9)	0.638
>20 mm	24 (54.5)	9 (69.2)	13 (59.1)	
Comedo necrosis				
No	26 (59.1)	3 (23.1)	5 (22.7)	0.005
Yes	18 (40.9)	10 (76.9)	17 (77.3)	
Histological grade				
Low	6 (13.6)	1 (7.6)	0 (0)	<0.001
Intermediate	19 (43.2)	6 (46.2)	1 (4.6)	
High	19 (43.2)	6 (46.2)	21 (95.4)	

ER: Estrogen receptor; PR: Progesterone receptor

Table 2. Mammographic findings of the lesions according to hormone receptor subgroups

	ER/PR positive (n) (%)	Single positive (n) (%)	ER/PR negative (n) (%)	p-value
Mammography findings				
Occult	9 (20.5)	0 (0)	6 (27.3)	0.348
Mass	11 (25)	3 (23.1)	6 (27.3)	
Microcalcification	17 (38.6)	9 (69.3)	7 (31.8)	
Microcalcification+mass	7 (15.9)	1 (7.6)	3 (13.6)	
Mass shape				
Round/ovoid	4 (22.2)	0 (0)	3 (33.3)	0.494
Lobular/irregular	14 (77.8)	4 (100)	6 (66.7)	
Mass margin				
Smooth circumscribed	1 (5.6)	0 (0)	1 (11.1)	1.000
Indistinct/spiculated	17 (94.4)	4 (100)	8 (88.9)	
Microcalcification morphology				
Amorphous	8 (33.4)	1 (10)	5 (50)	0.020
Course heterogeneous	2 (8.3)	2 (20)	2 (20)	
Fine pleomorphic	12 (50)	6 (60)	0 (0)	
Fine linear/fine linear branching	2 (8.3)	1 (10)	3 (30)	
Microcalcification distribution				
Regional	1 (4.2)	1 (10)	0 (0)	0.856
Grouped	12 (50)	4 (40)	4 (40)	
Linear	0 (0)	0 (0)	0 (0)	
Segmental	11 (45.8)	5 (50)	6 (60)	
MG-BI-RADS				
Category 4A	5 (14.3)	2 (15.4)	2 (12.6)	0.998
Category 4B	11 (31.4)	3 (23.1)	5 (31.2)	
Category 4C	11 (31.4)	5 (38.4)	5 (31.2)	
Category 5	8 (22.9)	3 (23.1)	4 (25)	

ER: Estrogen receptor; PR: Progesterone receptor; MG: Mammography; BI-RADS: Breast imaging reporting and data system

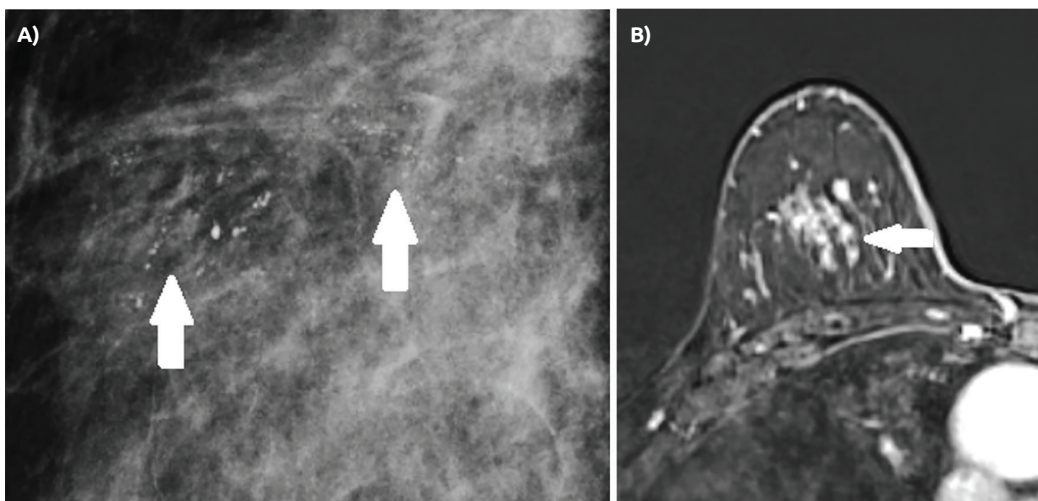


Figure 2. A 45-year-old woman with high-grade pure DCIS containing foci of comedo necrosis. Immunohistochemical analysis established that ER and PR were negative. **A.** A magnification view in the CC mammogram projection showed grouped amorphous calcifications (arrows). **B.** Axial postcontrast subtraction MRI image showed a clumped nonmass enhancement with focal distribution in the right breast (arrow)

DCIS: Ductal carcinoma in situ; ER: Estrogen receptor; PR: Progesterone receptor; CC: Craniocaudal; MRI: Magnetic resonance imaging

initial and delayed phase kinetic patterns is detailed in Table 3 and did not exhibit significant differences between the three groups ($p = 0.400$ and $p = 0.105$, respectively). The lesions were categorized as MRI BI-RADS 4 in 72% of the double HRc-positive group, 61% of the single HRc-positive group, and 81% of the double HRc-negative group. No statistically significant difference was found between receptor subgroups in terms of the MRI BI-RADS category ($p = 0.412$).

ADC Values

The median ADC value of DCIS lesions was $1323 \times 10^{-6} \text{mm}^2/\text{sec}$ in ER and PR-positive group, $1196 \times 10^{-6} \text{mm}^2/\text{sec}$ in single HRc-positive group and $1245 \times 10^{-6} \text{mm}^2/\text{sec}$ in the ER and PR-negative group. However, no significant relationship was observed between the lesion ADC value and HRc status ($p = 0.388$).

Table 3. DCE-MRI findings of the lesions according to hormone receptor subgroups

	ER/PR positive (n) (%)	Single positive (n) (%)	ER/PR negative (n) (%)	p-value
MRI findings				
Mass	7 (15.9)	1 (7.6)	4 (18.2)	0.831
NME	37 (84.1)	12 (92.4)	18 (81.8)	
Mass shape				
Round/ovoid	5 (71.4)	0 (0)	3 (75)	0.463
Lobular/irregular	2 (28.6)	1 (100)	1 (25)	
Mass margin				
Circumscribed	2 (28.6)	0 (0)	0 (0)	0.576
Irregular/spiculated	5 (71.4)	1 (100)	4 (100)	
Mass internal enhancement pattern				
Homogeneous	3 (42.8)	0 (0)	0 (0)	0.427
Heterogeneous	4 (57.2)	1 (100)	4 (100)	
Rim	0 (0)	0 (0)	0 (0)	
NME distribution				
Focal	12 (32.4)	5 (41.7)	3 (16.7)	0.042
Linear	2 (5.4)	0 (0)	7 (38.9)	
Segmental	16 (43.3)	6 (50)	6 (33.3)	
Regional	7 (18.9)	1 (8.3)	2 (11.1)	
Diffuse	0 (0)	0 (0)	0 (0)	
NME enhancement pattern				
Homogeneous	3 (8.1)	0 (0)	5 (27.8)	0.186
Heterogeneous	8 (21.6)	6 (50)	4 (22.2)	
Clumped	19 (51.4)	5 (41.7)	6 (33.3)	
Clustered ring	7 (18.9)	1 (8.3)	3 (16.7)	
Initial phase kinetic pattern				
Slow	14 (31.9)	3 (23.1)	6 (27.3)	0.400
Medium	13 (29.5)	7 (53.8)	5 (22.7)	
Rapid	17 (38.6)	3 (23.1)	11 (50)	
Delayed phase kinetic pattern				
Persistent	8 (18.2)	6 (46.2)	6 (27.2)	0.105
Plateau	26 (59.1)	3 (23.1)	8 (36.4)	
Washout	10 (22.7)	4 (30.7)	8 (36.4)	
MRI-BI-RADS				
Category 4	32 (72.7)	8 (61.5)	18 (81.8)	0.412
Category 5	12 (27.3)	5 (38.5)	4 (18.2)	

ER: Estrogen receptor; PR: Progesterone receptor; NME: Nonmass enhancement; DCE-MRI: Dynamic contrast-enhanced magnetic resonance imaging; BI-RADS: Breast imaging reporting and data system

The lesion-to-normal breast parenchyma ADC ratio showed notable variation across HRc status, being highest in double HRc-positive lesions (0.89) and lowest in double HRc-negative lesions (0.76). The ADC ratio demonstrated a significant association with the HRc status of DCIS lesions ($p = 0.033$) (Table 4). In the ROC curve analysis, the highest AUC [0.66 (0.53–0.78)] was obtained using an ADC ratio of 0.80 as the threshold, with corresponding sensitivity and specificity values of 66% and 65%, respectively (Figure 4).

Discussion and Conclusion

The current study assessed the predictive role of clinicopathological, MG, DCE-MRI features, and ADC values in determining the HRc status of pure DCIS lesions. Of the DCIS lesions in our study, 55% were histopathologically diagnosed as ER and PR-positive. This rate is slightly lower than that reported in a study with a larger patient population, where the rate of double HRc-positive cases was 68% (5). Hwang et al. (5) noted that younger mean patient ages were associated with ER and PR positivity compared to other DCIS subtypes. In our investigation, the relatively lower rate of HRc-positive cases was

considered to be associated with the older mean patient age in the study. Furthermore, the present study revealed that age was not a significant factor in predicting the HRc status of DCIS.

While DCIS is often asymptomatic, it can present with clinical symptoms such as a palpable mass, nipple discharge, or Paget’s disease (8, 17). Consistent with the literature, symptomatic DCIS cases were observed more frequently in the HRc-negative group in our study (17, 18). Rapid growth and progression leading to symptoms are associated with a poorer prognosis for DCIS (17, 18). HRc-positive DCIS lesions are known to have a tendency to increase slowly in size (4). In keeping with this, the smallest mean size among the three groups was observed in the HRc-positive group in our study. Therefore, it was not surprising that ER and PR-positive lesions were mostly asymptomatic. Comedo necrosis and high histological grade are considered aggressive histopathologic factors for DCIS lesions (19, 20). In the present study, these poor prognostic factors were observed at a higher rate in ER and PR-negative cases, consistent with previous studies in the literature (19, 21). The mentioned histopathologic features and the HRc status of the DCIS lesions showed a significant correlation.

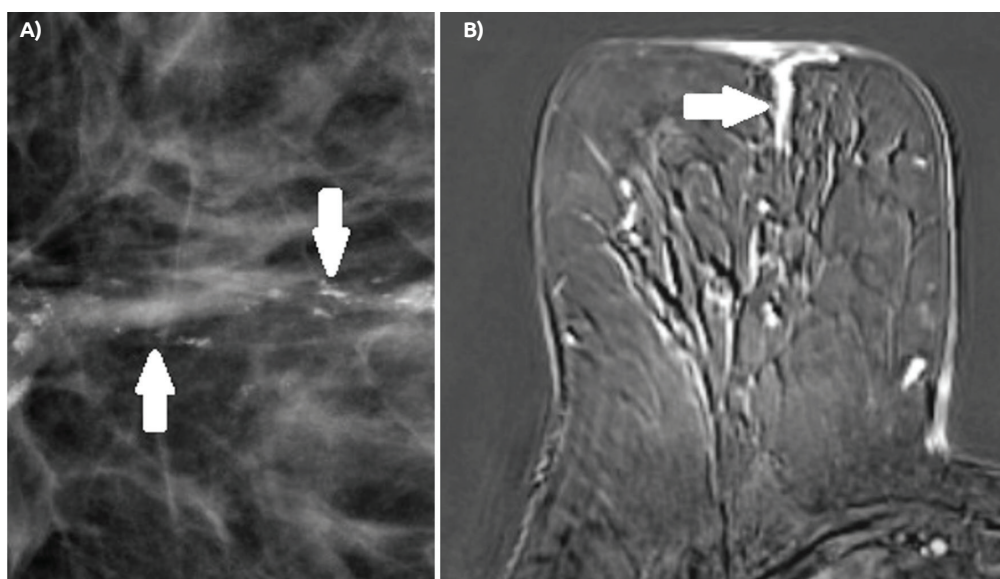


Figure 3. A 55-year-old woman with high-grade pure DCIS without comedo necrosis. Immunohistochemical analysis established that ER and PR were negative. **A.** A magnification view in the CC mammogram projection showed grouped fine pleomorphic and fine linear calcifications (arrows). **B.** Axial postcontrast subtraction MRI image showed a homogeneous nonmass enhancement with linear distribution in the right breast (arrow)

DCIS: Ductal carcinoma in situ; ER: Estrogen receptor; PR: Progesterone receptor; CC: Craniocaudal; MRI: Magnetic resonance imaging

Table 4. Comparison of patient’s age, lesion size, lesion ADC value, and lesion-to-normal breast parenchyma ADC ratio according to hormone receptor subgroups

	ER/PR positive (n) (%)	Single positive (n) (%)	ER/PR negative (n) (%)	p-value
Patient age (year) (mean ± SD)	49.59±10.07	47.31±9.34	55.86±15.89	0.150
Lesion size (mm) (median) (min-max)	23.5 (7–70)	36 (9–85)	35 (5–68)	0.240
Lesion ADC value (10 ⁻⁶ mm ² /sec) (median) (min-max)	1323 (1015–1699)	1196 (1005–1599)	1245 (976–1895)	0.388
Lesion/normal breast parenchyma ADC ratio (median) (min-max)	0.89 (0.63–0.99)	0.82 (0.66–0.95)	0.76 (0.66–0.98)	0.033

ER: Estrogen receptor; PR: Progesterone receptor; ADC: Apparent diffusion coefficient; SD: Standard deviation; Min: Minimum; Max: Maximum

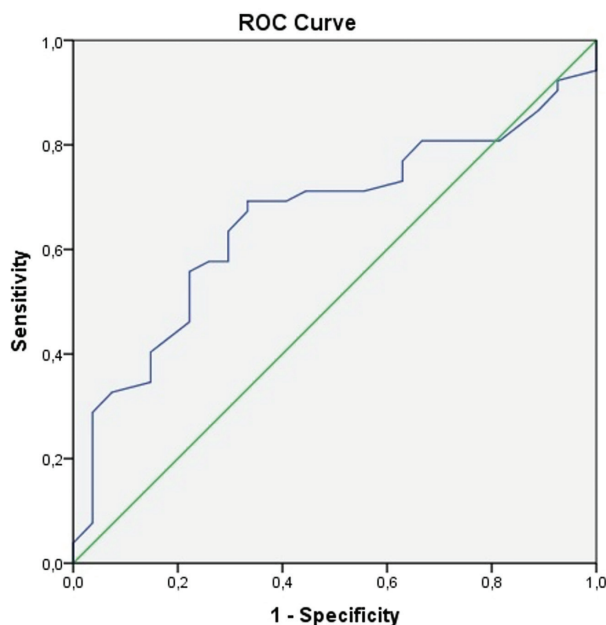


Figure 4. Graph shows ROC curve for differentiating double HRC positive DCIS from other HRC status of DCIS on the basis of lesion-to-normal breast parenchyma ADC ratio. The area under the ROC curve was 0.66 (95% CI: 0.53–0.78)

ROC: Receiver operating characteristic; HRC: Hormone receptor; DCIS: Ductal carcinoma in situ; ADC: Apparent diffusion coefficient CI: Confidence interval

Microcalcification is the predominant and prevalent manifestation of DCIS lesions in MG (2, 22, 23). The pathophysiology underlying calcification formation involves the concentration of mucin secretions within the duct/lobular acini or the calcification of endoluminal necrotic material, which comprises cell debris and excretions (24). The diversity in calcification morphologies and distributions stems from the variance in developmental mechanisms (2, 22). In the present study, a significant correlation was identified between calcification morphology and HRC status. In line with earlier published findings, the current investigation revealed that DCIS lesions with double and single positive-HRC were more frequently associated with fine pleomorphic calcifications, while ER and PR-negative DCIS lesions were more likely to exhibit amorphous calcifications (2, 19, 25). Moreover, across all three groups, the predominant distribution of calcifications was segmental and grouped, with no significant differences observed between the groups. This result is in keeping with those reported by Kim et al. (19). Of note, in previous studies that established a significant relationship between calcification distribution and receptor status, the number of cases in the receptor-negative group was notably low, potentially impacting the reliability of their results (2, 25).

In MG, the identification of DCIS lesions often hinges on the presence of suspicious calcifications. However, lesions devoid of calcification can also be encountered, rendering MG insufficient for DCIS diagnosis in such instances (26). Previous studies have reported the incidence of mammographically occult DCIS to range from 6% to 23% (8). Our study corroborates this trend, revealing a 19% rate, aligning with the existing literature. Given its high sensitivity for pure DCIS (77–96%), MRI proves valuable in accurately delineating the extent of the disease (6, 7). In MRI, the increased permeability of vascular and basement membranes in DCIS results in the accumulation of

gadolinium contrast agent in ducts and terminal lobules, leading to the most common presentation of DCIS on MRI as NME with a segmental or linear distribution (6, 14, 26). Our study concurs with these results, identifying NME as the most prevalent morphology across all three groups, in line with the literature. Moreover, HRC-positive lesions, both double and single, predominantly exhibited a segmental distribution, while HRC-negative lesions displayed a more frequent linear distribution on DCE-MRI. A notable correlation was established between the distribution of NME and the HRC status of the lesions. While previous studies have described typical enhancement patterns of DCIS lesions as clumped or heterogeneous, our investigation revealed a predominantly clumped pattern in both HRC-positive and -negative groups, with a heterogeneous pattern observed in the single HRC-positive group (7, 27). Notably, no association was identified between the enhancement pattern of the lesions and the groups. Kinetic data derived from DCE-MRI, when evaluated alongside other imaging data, can aid in the differential diagnosis of breast lesions. The kinetic curve of lesions, influenced by factors such as angiogenesis, leaky vasculature, cellularity, and changes in extracellular interstitial space, may vary for each lesion due to the contribution of these pathophysiological factors at different rates (15, 28).

Numerous prior studies have consistently identified the rapid initial phase with washout delayed phase enhancement as the prevailing kinetic pattern for DCIS (7, 27, 28). Our study showed a predominant display of a rapid initial enhancement with a plateau kinetic curve in DCIS lesions, echoing the results reported by Kim et al. (15). In a study by Bharti et al. (29), heightened microvessel proliferation was notably more common in ER-negative tumors. Building upon this insight, significant intergroup differences in the kinetic characteristics of DCIS lesions were initially anticipated in our investigation. Contrary to this expectation, our study revealed no discernible differences in the kinetic features of pure DCIS lesions based on HRC status.

DWI is an MRI technique that does not require a contrast agent, relying on the assessment of the random Brownian motion of water molecules within tissue (11, 13). The impedance of water molecular diffusion is influenced by the degree of tissue cellularity and the permeability of cell membranes (30). ADC serves as a quantifiable measure to evaluate this diffusion. ER and PR, and intranuclear receptors that impact DNA and participate in cell proliferation, may also influence the expression of aquaporins responsible for transporting water across cell membranes, thereby regulating tissue water diffusion (13). In the present study, ADC values for pure DCIS lesions were measured, with the aim of assessing their potential in discriminating HRC status. Rahbar et al. revealed similar ADC values for high nuclear grade and non-high nuclear grade DCIS lesions (11). Iima et al. (30) proposed that DCIS lesions with ADC values below 1.3 were likely to be low-grade. In addition, Rocknsharifi et al. (13) found lower ADC values in PR-negative breast cancer lesions, including DCIS and invasive tumors. While our results indicated a relatively lower ADC value in single HRC-positive pure DCIS lesions compared to other groups, our investigation ultimately found no significant difference in ADC values between the groups. To the best of our knowledge, no studies comparable to the current investigation have explored the correlation between ADC values and HRC status in DCIS. The variation in hormonal levels influences the water content in the interstitial area of breast tissue, as well as the proliferative activity of luminal epithelial cells and mitotic activity in breast lobules. Postmenopausal changes lead to a significant reduction in tissue water

content and cell proliferation. Consequently, ADC values in the breast parenchyma may vary significantly among individual patients (31, 32). Moreover, previous studies have established a correlation between decreased ADC in breast tumors and increased cellularity compared to normal fibroglandular tissue (10, 11). Recognizing this, it was posited that a more accurate assessment could be derived from the ratio of ADC values for DCIS lesions to normal breast parenchyma. Our study found that the lesion-to-normal breast parenchyma ADC ratio was associated with the HRc status of DCIS lesions. Thus it is suggested that the likelihood of double HRc positivity increased at values above 0.8, identified as the threshold. This observation aligned with our discovery that the ER and PR-positive group exhibited the highest ADC values.

Several limitations were inherent in our study. Firstly, the retrospective nature and the single-center design with a limited sample size may impact the generalizability of our results. Future research endeavors should focus on multicenter prospective investigations involving larger patient cohorts to validate our results and uncover potential new associations. Secondly, our inclusion criteria, which involved cases undergoing preoperative MG and MRI, may introduce selection bias. Cases with dense artifacts in DWI images and very small lesions (<5 mm) were excluded, potentially limiting the representativeness of our results for all DCIS lesions. Thirdly, the heterogeneous internal structure of DCIS lesions posed challenges in standardizing kinetic evaluation and ADC measurements. Fourthly, in our study HER-2 expression, which is indicated in the literature as a prognostic factor for recurrence of DCIS lesions and response to radiotherapy, was not investigated (33, 34). The reason for this is that HER-2 expression is not routinely evaluated in DCIS at our center. Finally, the retrospective interpretation of MG and MRI images by a single radiologist may introduce variability, given the morphological intralesional heterogeneity of DCIS. Different outcomes might have been observed if multiple radiologists had evaluated the images.

In conclusion, our study identified clinicopathological features such as the presence of symptoms and comedo necrosis, and high histological grade, along with amorphous microcalcifications and the linear distribution pattern of NME, as potential indicators for HRc-negativity in DCIS. Furthermore, a lesion-to-normal parenchyma ADC ratio threshold of 0.80 was established as predictive for ER and PR-positive DCIS lesions. To the best of our knowledge, no study in the literature has investigated MRI features based on HRc status in pure DCIS lesions, making our study a potential guide in this unexplored area.

Ethics Committee Approval: This retrospective study received approval from the Non-Interventional Clinical Research Ethics Committee of Health Sciences University Turkey, Dr. Abdurrahman Yurtaslan Ankara Oncology Health Education Application and Research Center (no.: 2023-12/123, date: 14.12.2023).

Informed Consent: Informed consent was obtained from each participant.

Authorship Contributions

Surgical and Medical Practices: A.C.B., Z.M.B.; Concept: A.C.B.; Design: A.C.B., Z.M.B.; Data Collection and/or Processing: A.C.B., Z.M.B.; Analysis and/or Interpretation: A.C.B.; Literature Search: A.C.B.; Writing: A.C.B.

Conflict of Interest: The authors have no conflicts of interest to declare.

Financial Disclosure: The authors declared that this study has received no financial support.

References

- Villanueva H, Grimm S, Dhamne S, Rajapakshe K, Visbal A, Davis CM, et al. The Emerging Roles of Steroid Hormone Receptors in Ductal Carcinoma in Situ (DCIS) of the Breast. *J Mammary Gland Biol Neoplasia*. 2018; 23: 237-248. (PMID: 30338425) [[Crossref](#)]
- Avdan Aslan A, Gültekin S, Esendağlı Yılmaz G, Kurukahvecioğlu O. Is There Any Association Between Mammographic Features of Microcalcifications and Breast Cancer Subtypes in Ductal Carcinoma In Situ? *Acad Radiol*. 2021; 28: 963-968. (PMID: 32620528) [[Crossref](#)]
- Stanciu-Pop C, Nolleaux MC, Berlière M, Duhoux FP, Fellah L, Galant C, et al. Morphological intratumor heterogeneity in ductal carcinoma in situ of the breast. *Virchows Arch*. 2021; 479: 33-43. (PMID: 33502600) [[Crossref](#)]
- Tay THC, Ng WY, Ong KW, Wong CY, Tan BKT, Yong WS, et al. Impact of hormonal status on ductal carcinoma in situ of the breast: Outcome and prognostic factors. *Breast J*. 2020; 26: 937-945. (PMID: 31876337) [[Crossref](#)]
- Hwang KT, Suh YJ, Park CH, Lee YJ, Kim JY, Jung JH, et al. Hormone Receptor Subtype in Ductal Carcinoma in Situ: Prognostic and Predictive Roles of the Progesterone Receptor. *Oncologist*. 2021; 26: e1939-e1950. (PMID: 34402131) [[Crossref](#)]
- Grimm LJ, Rahbar H, Abdelmalak M, Hall AH, Ryser MD. Ductal Carcinoma in Situ: State-of-the-Art Review. *Radiology*. 2022; 302: 246-255. (PMID: 34931856) [[Crossref](#)]
- Jansen SA, Newstead GM, Abe H, Shimauchi A, Schmidt RA, Karczmar GS. Pure ductal carcinoma in situ: kinetic and morphologic MR characteristics compared with mammographic appearance and nuclear grade. *Radiology*. 2007; 245: 684-691. (PMID: 18024450) [[Crossref](#)]
- Shin HJ, Kim HH, Kim SM, Kwon GY, Gong G, Cho OK. Screening-detected and symptomatic ductal carcinoma in situ: differences in the sonographic and pathologic features. *AJR Am J Roentgenol*. 2008; 190: 516-525. (PMID: 18212241) [[Crossref](#)]
- Benveniste AP, Ortiz-Perez T, Ebuoma LO, Sepulveda KA, Severs FJ, Roark A, et al. Is breast magnetic resonance imaging (MRI) useful for diagnosis of additional sites of disease in patients recently diagnosed with pure ductal carcinoma in situ (DCIS)? *Eur J Radiol*. 2017; 96: 74-79. (PMID: 29103479) [[Crossref](#)]
- Greenwood HI, Wilmes LJ, Kelil T, Joe BN. Role of Breast MRI in the Evaluation and Detection of DCIS: Opportunities and Challenges. *J Magn Reson Imaging*. 2020; 52: 697-709. (PMID: 31746088) [[Crossref](#)]
- Rahbar H, Partridge SC, Eby PR, Demartini WB, Gutierrez RL, Peacock S, et al. Characterization of ductal carcinoma in situ on diffusion weighted breast MRI. *Eur Radiol*. 2011; 21: 2011-2019. (PMID: 21562806) [[Crossref](#)]
- Arnedos M, Nerurkar A, Osin P, A'Hern R, Smith IE, Dowsett M. Discordance between core needle biopsy (CNB) and excisional biopsy (EB) for estrogen receptor (ER), progesterone receptor (PgR) and HER2 status in early breast cancer (EBC). *Ann Oncol*. 2009; 20: 1948-1952. (PMID: 19570962) [[Crossref](#)]
- Roknsharif S, Fishman MDC, Agarwal MD, Brook A, Kharbanda V, Dialani V. The role of diffusion weighted imaging as supplement to dynamic contrast enhanced breast MRI: Can it help predict malignancy,

- histologic grade and recurrence? *Acad Radiol.* 2019; 26: 923-929. (PMID: 30293819) [\[Crossref\]](#)
14. Liu H, Peng W. MRI morphological classification of ductal carcinoma in situ (DCIS) correlating with different biological behavior. *Eur J Radiol.* 2012; 81: 214-217. (PMID: 21296513) [\[Crossref\]](#)
 15. Kim JA, Son EJ, Youk JH, Kim EK, Kim MJ, Kwak JY, et al. MRI findings of pure ductal carcinoma in situ: kinetic characteristics compared according to lesion type and histopathologic factors. *AJR Am J Roentgenol.* 2011; 196: 1450-1456. (PMID: 21606313) [\[Crossref\]](#)
 16. Morris EA, Comstock CE, Lee CH. ACR BI-RADS®. In: ACR BI-RADS® Atlas, Breast imaging reporting and data system. Reston, VA: American College of Radiology. 2013:56-71. [\[Crossref\]](#)
 17. Barnes NL, Dimopoulos N, Williams KE, Howe M, Bundred NJ. The frequency of presentation and clinico-pathological characteristics of symptomatic versus screen detected ductal carcinoma in situ of the breast. *Eur J Surg Oncol.* 2014; 40: 249-254. (PMID: 24433818) [\[Crossref\]](#)
 18. Koh VC, Lim JC, Thike AA, Cheok PY, Thu MM, Tan VK, et al. Characteristics and behaviour of screen-detected ductal carcinoma in situ of the breast: comparison with symptomatic patients. *Breast Cancer Res Treat.* 2015; 152: 293-304. (PMID: 26077641) [\[Crossref\]](#)
 19. Kim MY, Kim HS, Choi N, Yang JH, Yoo YB, Park KS. Screening mammography-detected ductal carcinoma in situ: mammographic features based on breast cancer subtypes. *Clin Imaging.* 2015; 39: 983-986. (PMID: 26259866) [\[Crossref\]](#)
 20. Moon HJ, Kim EK, Kim MJ, Yoon JH, Park VY. Comparison of Clinical and Pathologic Characteristics of Ductal Carcinoma in Situ Detected on Mammography versus Ultrasound Only in Asymptomatic Patients. *Ultrasound Med Biol.* 2019; 45: 68-77. (PMID: 30322671) [\[Crossref\]](#)
 21. Barnes NL, Boland GP, Davenport A, Knox WF, Bundred NJ. Relationship between hormone receptor status and tumour size, grade and comedo necrosis in ductal carcinoma in situ. *Br J Surg.* 2005; 92: 429-434. (PMID: 15736216) [\[Crossref\]](#)
 22. Tang X, Yamashita T, Hara M, Knox WF, Bundred NJ. Histopathological characteristics of breast ductal carcinoma in situ and association with imaging findings. *Breast Cancer.* 2016; 23: 491-498. (PMID: 15736216) [\[Crossref\]](#)
 23. Kim JH, Ko ES, Kim DY, Han H, Sohn JH, Choe DH. Noncalcified ductal carcinoma in situ: imaging and histologic findings in 36 tumors. *J Ultrasound Med.* 2009; 28: 903-910. (PMID: 19546332) [\[Crossref\]](#)
 24. Henrot P, Leroux A, Barlier C, Génin P. Breast microcalcifications: the lesions in anatomical pathology. *Diagn Interv Imaging.* 2014; 95: 141-152. (PMID: 24525087) [\[Crossref\]](#)
 25. Bae MS, Moon WK, Chang JM, Cho N, Park SY, Won JK, et al. Mammographic features of calcifications in DCIS: correlation with oestrogen receptor and human epidermal growth factor receptor 2 status. *Eur Radiol.* 2013; 23: 2072-2078. (PMID: 23512196) [\[Crossref\]](#)
 26. Scott-Moncrieff A, Sullivan ME, Mendelson EB, Wang L. MR imaging appearance of noncalcified and calcified DCIS. *Breast J.* 2018; 24: 343-349. (PMID: 29139591) [\[Crossref\]](#)
 27. Chan S, Chen JH, Agrawal G, Lin M, Mehta RS, Carpenter PM, et al. Characterization of Pure Ductal Carcinoma In Situ on Dynamic Contrast-Enhanced MR Imaging: Do Nonhigh Grade and High Grade Show Different Imaging Features? *J Oncol.* 2010; 2010: 431341. (PMID: 20885929) [\[Crossref\]](#)
 28. Chen ST, Covelli J, Okamoto S, Daniel BL, DeMartini WB, Ikeda DM. Clumped vs non-clumped internal enhancement patterns in linear non-mass enhancement on breast MRI. *Br J Radiol.* 2021; 94: 20201166. (PMID: 33332980) [\[Crossref\]](#)
 29. Bharti JN, Rani P, Kamal V, Agarwal PN. Angiogenesis in Breast Cancer and its Correlation with Estrogen, Progesterone Receptors and other Prognostic Factors. *J Clin Diagn Res.* 2015; 9: EC05-EC07. (PMID: 25737993) [\[Crossref\]](#)
 30. Iima M, Le Bihan D, Okumura R, Okada T, Fujimoto K, Kanao S, et al. Apparent diffusion coefficient as an MR imaging biomarker of low-risk ductal carcinoma in situ: a pilot study. *Radiology.* 2011; 260: 364-372. (PMID: 21633054) [\[Crossref\]](#)
 31. Mori N, Mugikura S, Takasawa C, Miyashita M, Shimauchi A, Ota H, et al. Peritumoral apparent diffusion coefficients for prediction of lymphovascular invasion in clinically node-negative invasive breast cancer. *Eur Radiol.* 2016; 26: 331-339. (PMID: 26024846) [\[Crossref\]](#)
 32. Ramakrishnan R, Khan SA, Badve S. Morphological changes in breast tissue with menstrual cycle. *Mod Pathol.* 2002; 15: 1348-1356. (PMID: 12481017) [\[Crossref\]](#)
 33. Yang L, Shen M, Qiu Y, Tang T, Bu H. Molecular subtyping reveals uniqueness of prognosis in breast ductal carcinoma in situ patients with lumpectomy. *Breast.* 2022; 64: 1-6. (PMID: 35462343) [\[Crossref\]](#)
 34. Thorat MA, Levey PM, Jones JL, Pinder SE, Bundred NJ, Fentiman IS, et al. Prognostic and Predictive Value of HER2 Expression in Ductal Carcinoma In Situ: Results from the UK/ANZ DCIS Randomized Trial. *Clin Cancer Res.* 2021; 27: 5317-5324. (PMID: 34380636) [\[Crossref\]](#)